Life Sciences 184 (2017) 47–57

Contents lists available at ScienceDirect

Life Sciences

journal homepage: www.elsevier.com/locate/lifescie

Effects of Huperzin-A on the Beta-amyloid accumulation in the brain and skeletal muscle cells of a rat model for Alzheimer's disease

Cagatay Han Turkseven [a], Belgin Buyukakilli [a,*], Ebru Balli [b], Derya Yetkin [b], Mehmet Emin Erdal [c], Senay Gorucu Yilmaz [c], Leyla Sahin [d]

[a] Department of Biophysics, Faculty of Medicine, Mersin University, Mersin, Turkey
[b] Department of Histology & Embryology, Faculty of Medicine, Mersin University, Mersin, Turkey
[c] Department of Medical Biology, Faculty of Medicine, Mersin University, Mersin, Turkey
[d] Department of Physiology, Faculty of Medicine, Mersin University, Mersin, Turkey

ARTICLE INFO

Article history:
Received 21 January 2017
Received in revised form 19 June 2017
Accepted 10 July 2017
Available online 12 July 2017

Keywords:
Alzheimer's disease
β-amyloid peptide
Motor dysfunction
Electromyography
Huperzine-a
Inclusion body myositis

ABSTRACT

Aims: Alzheimer's Disease (AD) is characterized by a loss of cognitive function and also the accumulation of β-amyloid peptide (βAP) in the brain parenchyma, which plays an important role in this disease. However, it is often also associated with the non-cognitive symptoms such as loss of muscle function (Inclusion-Body Myositis-IBM).
Main methods: Sprague-Dawley rats (13 weeks-n = 68) were randomly assigned into five groups: Group C: Control; Group D: D-galactose; Group O + D: Bilateral oophorectomy + D-galactose; Group O: Bilateral oophorectomy; Group O + D + H: Bilateral oophorectomy + D-galactose + Hup-A. Tissue fixation was performed with the perfusion method. The Compound Muscle Action Potential (CMAP) and mechanical muscle activity were recorded using the standard electro-biophysical techniques. Immune staining was performed with specific antibodies, and the pathological changes were examined. RNA was obtained from brain tissue samples with the Trizol Method. Then, the expression data of mature-miRNAs (*rno-miR-9-5p, rno-miR-29a-3p, rno-miR-106a-5p, rno-miR-107 and rno-miR-125a-3p*), which may be effective in AD, were taken with Real-Time PCR.
Key findings: Impairments occurred in behavioral tests of the rats in the O + D group. βAP accumulation and AChE activity increased significantly in the forebrain in the O + D group compared to the C group. It was seen that Huperzine-A (Hup-A) reduced AChE activity and destructed βAP accumulation. There was a significant decrease in the maximum contractile force at different frequencies in the O + D group and in the O group compared to the C group.
Significance: It was found that Hup-A contributed to the healing process in rats for damage occurring both in the brain and in the neuro-muscular system.

1. Introduction

Alzheimer's Disease (AD) leads to neuronal death due to the excessive accumulation of β-amyloid peptide (βAP) in the extracellular tissue and of neurofibrillary tangles in the intracellular tissue as a result of the loss of the cholinergic neurons in the brain's frontal cortex and the hippocampus [1–2].

Another pathological finding in AD except for cognitive impairments is the loss of muscle functions. Kuo et al. [3] found for the first time that there was an increase in the aggregation of Aβ40 and Aβ42 peptide forms in the temporal muscles in patients with AD dementia compared to healthy controls. Thus, they showed that the changes in β-amyloid-precursor protein and βAP metabolism might also occur in peripheral tissues [3]. In the studies conducted in patients with Inclusion-Body Myositis (IBM), which is considered to share the same etiology with AD, the presence of βAP accumulation and phosphorylated tau protein was shown in both muscle biopsy and brain tissue [4–5]. In a study performed using conventional electro-biophysical techniques to investigate the effect of βAP and its mechanisms on the resting membrane potential of skeletal muscle fibers of the frog, it was shown that βAP disrupted the resting membrane potential of skeletal muscle fibers by leading to a marked depolarization on skeletal muscle plasma membrane and also this was due to both the inhibition of Na+/K+-ATPase and the formation of βAP-pores. The formation of βAP-pores leads to an increase in the membrane permeability. It is considered that the depolarization of skeletal muscle plasma membrane induced by βAP can disrupt significantly the functions of skeletal muscle [6–8].

MicroRNAs (miRNA)'s contribution to sporadic AD is not clear. It was found that several miRNAs are significantly altered in AD. Expression

* Corresponding author.
E-mail address: bbuyukakilli@yahoo.com (B. Buyukakilli).

http://dx.doi.org/10.1016/j.lfs.2017.07.012
0024-3205/

levels of genes appeared to have decreased in the brain tissue of AD patients [9].

It is known that Hup-A serves as a cholinesterase inhibitor which enhances neurotransmitter levels in the brain [10]. There is still a need for new studies on this subject. Huperzine-A shows the effect on the peripheral and central nervous system by blocking acetylcholinesterase. After it is rapidly absorbed from the blood-brain barrier, it distributes to all body [11]. This effect suggests that it can be effective on the expression of the down-regulated miRNAs in the brain.

In the literature, although there are many studies about the deterioration of the electrical mechanism of skeletal muscle fiber membranes due to AD, there is no any study investigating the effect of AD on the mechanical activity of skeletal muscle.

The purpose of this study is to examine effects of AD on contractility of skeletal muscle and to contribute to the information available on the mechanisms of skeletal muscle dysfunction and motor disturbances due to AD with the obtained results. Furthermore, we hypothesize that Hup-A, with potentially disease-modifying qualities in AD, may have an important role in skeletal muscle mechanical activity in AD modeling. It developed as based on a long-term administration of D-galactose following the formation of menopause. Hup-A is a potential drug which is used for AD treatment and it was applied in the rat model used in this study and then their effects on the brain and skeletal muscle functions were examined. Moreover, the relationship between Hup-A and the expression levels of miRNAs was investigated, and its role in the mechanism of miRNA during the treatment period was shown.

2. Materials and methods

2.1. Animals

Sixty-eight healthy adult female Sprague-Dawley rats (13 weeks old and average body weight 180–200 g) were used in this study. The rats were obtained from the Experimental Animal Center, Guinea-Pig Laboratory of Ankara, Turkey. The study was approved by the Research and Ethical Committee of the University of Mersin. The rats were housed in polycarbonate boxes (three or four rats per box) with steel wire tops and rice husk bedding. They were maintained in a controlled atmosphere of 12 h dark/light cycle, at 22 ± 2 °C temperature, and at 50–70% humidity, with free access to pelleted feed and fresh tap water. The animals were supplied with dry food pellets commercially available. The animals were randomly assigned into five groups: Group C (the Control Group-12 rats), Group D (D-galactose, 100 mg/kg/day-14 rats), Group O + D (bilateral oophorectomy-(OVX), D-galactose 100 mg/kg/day-14 rats), Group O (bilateral oophorectomy-(OVX)-14 rats) and Group O + D + H (bilateral oophorectomy-(OVX), D-galactose 100 mg/kg/day, Huperzine-A 0,1 mg/kg/day-14 rats).

2.2. Experimental protocol

After the rats in the O + D + H group underwent bilateral ovariectomy, D-galactose (100 mg/kg/day in 9% saline, i.p. injection every day) was applied for 10 weeks; and Hup-A (0,1 mg/kg/day in 9% saline, i.p. injection every day) was applied for 3 weeks from the 8th week following one recovery week. The same experimental procedure except for Hup-A injection in the O + D + H group was performed in the rats in the O + D group. The incision was opened and closed on the *linea alba* without excising the ovaries of the rats in the D group and D-galactose; and 9% saline (i.p.) injection were applied as in the O + D + H group following recovery. After the rats in the O group underwent bilateral ovariectomy, 9% saline (i.p.) injection was applied. The rats in the C group were given D-galactose and 9% saline (i.p.) injection within Hup-A every day for 11 weeks.

2.3. Behavioral tests

The open field and the Morris water maze tests were performed respectively in 27 weeks to evaluate spatial memory ability and learning and locomotor activity. The procedures for these behavioral tests were made as previously reported and briefly defined below [12–14]. All experiments were recorded by the Noldus Ethovision XT software with the computer system and the digital camera.

2.3.1. Open field test

Locomotor activity of the rats was observed in the area where there is bright light (100 cm diameter closed by a wall 40 cm high). The rats were placed in the center of the open-field and the test was started. The distance (cm) covered in five minutes on the floor by them and their movement speeds (cm/s) were recorded.

2.3.2. Morris water maze testing

The Morris water maze ($R = 150$ cm diameter, $h = 60$ depth) was used to examine the effects of the applications on learning and spatial memory. In short, it was observed with the computer system and the digital camera that the rats were looking for the platform in any time period. Four attempts were made every day for four consecutive days. The platform was removed on the 5th day and each rat was allowed to swim freely for 60 s and then the probe test was completed. At the end of this period, the time spent by them and their swimming speeds at the quadrant where the platform was formerly were recorded.

2.4. Tissue preparation

After the behavioral tests, each group was divided in two for electrobiophysics and histopathological examinations. They were anesthetized by applying 80 mg/kg Ketamine HCl (Ketalar® flakon, Parke-Davis, ESA) and 10 mg/kg xylazine HCl (Rompun flk, Bayer, Turkey) i.p. They were placed in the supine position on the electrically heated AOT0801-DC Animal Operating Table (DC-Heated Animal Operating Table-MAY QOT08019). Rectal temperature was allowed to keep at 37–38 °C for electrical records to be taken from the EDL muscle of the left leg. The EDL muscle of the right leg was removed from mechanical records. One end was connected to isometric force transducer (FDT 05 Force Displacement Transducer) with 2–0 silk sutures bound to the tendons of the isolated EDL muscle, and the other end was connected by placing in the organ bath which contained 10 ml of Krebs solution and was kept at 37 °C; and then it was maintained under these conditions until the record was received. A mixture of 4% paraformaldehyde and 0.05% glutaraldehyde within 9% cold saline was perfused into the rats for immunohistochemical examinations. The brain tissues including the cerebral cortex and the hippocampus and also the EDL muscle were removed. The tissues were allowed to be fixed in formaldehyde for immunohistochemical examinations [13]. The brain tissues were stored at −80 °C for genetic analysis.

2.5. Electro-biophysical tests

2.5.1. Electrical activity properties of EDL muscles

The Compound Motor Action Potentials (CMAP) were recorded in all groups using the standardized nerve conduction study techniques [15]. The data were collected by means of a BIOPAC® MP 100 acquisition system (Santa Barbara, USA). Bipolar surface electrodes (Medelec® small bipolar nerve electrodes, 6984 T, Oxford, UK) were used for stimulation. Surface disc electrodes (Medelec®, number 017 K006, Oxford, UK) were used for CMAP recordings from the EDL muscle. The ground electrode was placed on the thigh on the side of stimulation. The supramaximal stimulus consisted of single square pulse (duration 0,5 ms). BIOPAC Acknowledge Analysis software® (ACK 100 W) was used to measure CMAP peak-to-peak amplitude, peak latency, total duration, depolarization duration, 50% repolarization duration, amplitude and area.

2.5.2. Contractile properties of EDL muscles

Isolated organ bath (Isolated Organ Bath Stand Set-IOB S99) and isometric force transducer (FDT 05 Force Displacement Transducer) were used in recording the mechanical responses of the EDL. Isometric force transducer output was connected to the amplifier module (MAY-GTA-200) on the BIOPAC MP100 system (BIOPAC MP100 Systems Inc., Santa Barbara, USA). The content of the Krebs solution (mM/L) in the organ bath consisted of NaCl (118 mM), KCl (4.8 mM), $MgSO_4$ (1.2 mM), KH_2PO_4 (1.2 mM), glucose (10 mM), $NaHCO_3$ (23.7 mM), $CaCl_2$ (2.5 mM). The EDL muscle was placed between two platinum wire electrodes. The electrodes were directly contacted to the tissue. Bath solution was kept at 37 °C with a heating circulator (Heating Circulator/Model MAY WBC 3044-PR) which enables to control the temperature and also it was continuously gassed with a mixture of 95% O2 and 5% CO2. The Krebs Solution where the EDL muscle was placed was replaced every 15 min and the muscle was incubated in this medium for 30 min in order to balance it by adapting the bathroom environment [16–17]. After the equilibration period in the Krebs Solution, prestress values which bring each EDL muscle to the optimal length (L_0) were measured before isometric force responses formed by each EDL muscle for stimuli at different frequencies (1, 10, 20, 40, 80, 100 and 150 Hz) were recorded. Moreover, appropriate prestress values which bring the muscle preparation to the optimal length were adjusted by means of a micrometer attached to one end of the muscle before each alert protocol was applied. The maximum alert output of the stimulator on the BIOPAC MP100 system was ± 5 V. This value was found not to be a suitable range for supramaximal stimulus voltage required to induce muscles. Therefore, the stimulator (STM 100-EXT STIM) on the BIOPAC MP100 system was connected to a stimulus isolator (MAY-ISO150-A Serial No: 200,001–1 Stimulus Isolated Power Supply) which can be adjusted up to the output voltage of 150 V and then preliminary trials were performed; and it was observed that the EDL muscle reached the supramaximal amplitude with about 40 V. Thus, the amplitude of the stimulus voltage was used as 40 V in order to obtain the records of mechanical activity at the supramaximal amplitude in the EDL muscles during the study. Stimuli at different frequencies (1, 10, 20, 40, 80, 100 and 150 Hz) were given with an interval of 5 min for the EDL muscles which were brought to the optimal length (L_0), and the mechanical responses of the muscle were recorded on the data recording and analysis system (BIOPAC MP100 Systems Inc. Santa Barbara, USA) which transfers the responses transmitted through isometric force transducer to the computer via difference amplifier. The maximum contraction force (N) was normalized to be divided by the cross sectional area (cm^2) (CSA) (Fig. 1).

2.6. Immunohistochemistry

The rats were deeply anesthetized with ketamine HCl (Ketalar) 80 mg/kg and xylazine HCl (Rompun) 10 mg/kg i.p. and then killed by transcardial perfusion with cold 0.9% saline followed by 4% paraformaldehyde (pH 7.4). The tissue samples were removed and fixed in neutral formalin before dehydrating in a graded series of alcohols, cleared in xylene and embedded in paraffin. Five micrometer sections were cut from paraffin-embedded tissue blocks onto adhesive coated slides for immunohistochemistry. Sections were dewaxed (xylene 2 × 3 min) and rehydrated by passing through graded alcohol and rinsed with distilled water. Endogenous peroxidase activity was blocked with 3% hydrogen peroxide in methanol for 10 min. Nonspecific binding sites were blocked using a commercially available blocking solution for 10 min at room temperature. Afterwards, 1/50 diluted rabbit polyclonal Ig G anti-Aβ (Abcam, RabMab, USA) and mouse monoclonal anti-AChE (Abcam, RabMab, USA) primary antibody in PBS containing 5‰ bovine serum albumin solution was dropped on the sections, and then the sections were incubated for overnight at + 4 °C. The following day, biotinylated Goat Anti-Polyvalent secondary antibody solution was dropped on the sections, and then the sections were incubated for 10 min at room temperature. They were incubated for additional 20 min with streptavidinperoxidase enzyme reagent and were then washed. Finally, peroxidase substrate diaminobenzidin (DAB) was dropped and they were incubated for 1 min while the staining intensity was checked under the microscope. The sections were washed with distilled water for 5 min and counterstained with hematoxylin. On the sections separated for negative control, diluting buffer with no primary antibody was dropped.

$$\frac{\text{Maximum contraction force } (N)}{CSA\,(cm^2)} = \frac{N}{\text{Muscle mass } (g) \Big/ L_0\,(cm) \times 1.056\,(g/cm^3)}$$

Fig. 1. The maximum contraction force (N) obtained from isometric oscillation curves was normalized according to the cross sectional area (CSA) and was evaluated. The cross sectional area (CSA) was calculated with the above formula by accepting the muscle density as 1.056 g/cm^3.

2.6.1. Light microscopic evaluation

At the light microscopic level, the aggregates formed by Aβ peptides and AChE activity in brain tissue were investigated to be marked using rabbit polyoclonal Ig G anti-Aβ (Abcam, RabMab, USA) and mouse monoclonal anti-AChE (Abcam, RabMab, USA) antibodies by immunohistochemical labeling, and then they were evaluated in terms of staining intensity.

2.7. RNA extraction

RNA was extracted from the whole brain tissue using the modified method of Trizol® [18].

2.7.1. Reverse transcriptase PCR reactions (RT-PCR)

cDNAs were obtained from each RNA sample. Reverse transcriptase reactions contained 5 μl of extracted total RNA, 50 nM stem–loop RT primer, 1× RT buffer, 0.25 mM each of dNTPs, 50 units of modified M-MuLV Reverse Transcriptase (Thermo Scientific, Vilnius, Lithuania), 25 units of RiboLock RNase inhibitor (Thermo Scientific, Vilnius, Lithuania) and nuclease-free water to a total reaction volume of 15 μl. The reaction was performed on an automated Thermal Cycler (TechneFlexigene, Cambridge, UK). RT-PCR conditions are as follows; keeping for 30 min at 16 °C; for 30 min at 42 °C; for 5 min at 85 °C and then held at 4 °C.

2.7.2. Quantitative-Comparative CT (ΔΔCT) Real-Time PCR

Quantitative-Comparative CT (ΔΔCT) Real-Time PCR was performed in an ABI Prism 7500 Real-Time PCR System (Applied Biosystems, Foster City, CA, USA) using the SDS 2.0.6 software. The specific primers and fluorogenic ZNA™ probes for the miRNAs were designed using Primer Express 3.0 software (Applied Biosystems), and are listed in Table 1. The rno-miR-26b-5p was used as an endogenous control miRNA. The mixed RNAs created from the Control Group were used as a Reference RNA sample. Primers and probes were purchased from Metabion International AG, D-82152 Martinsried/Deutschland. The 25 μl PCR included 3 μl RT-PCR products, 12.5 μl of 2× TaqMan Universal PCR Master Mix (Applied Biosystems), 900 nmol of each primer (Primer F and Universal Primer R) and 200 nmol TaqMan® probe. The reactions were incubated in a 96-well plate of preincubation at 50 °C for 2 min and at 95 °C for 10 min followed by 40 cycles at 95 °C for 15 s and at 60 °C for 90 s. Amplifications and analyses were performed in an ABI Prism 7500 Real-Time PCR System (Applied Biosystems), using the SDS 2.0.6 software for allelic discrimination (Applied Biosystems). All reactions were performed in a triplicate manner. The expression levels of miRNAs in the

Table 1
List of the miRNAs characterized, the RT-PCR and Real-Time PCR primer-probe sequences utilized in the experiments.

miRNA	miRNA ID[a]	miRNA sequence ID[b]	Primer and probe sequences
rno-miR-26b-5p	407017	NR_029500.1	5′-RT-GTCGTATGCAGTGCAGGGTCCGAGGTATTCGCACTGCATACGACACCTAT-3′ 5′-F-GCCGCTTCAAGTAATTCAGG-3′ 5′-PR-FAM-TG(pdC)ATA(pdC)GA(pdC)A(pdC)CTATCC-ZNA4-BHQ-1-3′
rno-miR-9-5p	407046 NR_029691.1		5′-RT-GTCGTATGCAGTGCAGGGTCCGAGGTATTCGCACTGCATACGACTCATAC-3′ 5′-F-GCCGCTCTTTGGTTATCTAGCT-3′ 5′-PR-FAM- TG(pdC)ATA(pdC)GA(pdC)T(pdC)ATA(pdC)AG-ZNA4-BHQ1–3′
rno-miR-29a-3p	407021 NR_029503.1		5′-RT-GTCGTATGCAGTGCAGGGTCCGAGGTATTCGCACTGCATACGACTAACCG-3′ 5′-F-GCCGCTAGCACCATCTGAAAT-3′ 5′-PR-FAM- TG(pdC)ATA(pdC)GA(pdC)TAA(pdC)CGAT-ZNA4-BHQ1–3′
rno-miR-106a-5p	406899 NR_029523.1		5′-RT-GTCGTATGCAGTGCAGGGTCCGAGGTATTCGCACTGCATACGACCTACCT-3′ 5′-F-GCCGCAAAAGTGCTTACAGTGC-3′ 5′-PR-FAM- TG(pdC)ATA(pdC)GA(pdC)CTACCTGC-ZNA4-BHQ1–3′
rno-miR-107	406901	NR_029524.1	5′-RT-GTCGTATGCAGTGCAGGGTCCGAGGTATTCGCACTGCATACGACTGATAG-3′ 5′-F-GCCGCAGCAGCATTGTACAGGG-3′ 5′-PR-FAM- TG(pdC)ATA(pdC)GA(pdC)TGATAG(pdC)C-ZNA4-BHQ-1-3′
rno-miR-125a-3p	406910	NR_029693.1	5′-RT-GTCGTATGCAGTGCAGGGTCCGAGGTATTCGCACTGCATACGACGGCTCC-3′ 5′-F-GCCGCACAGGTGAGGTTCTTG-3′ 5′-PR-FAM-TGCATACGACGGCTCCCA-ZNA4-BHQ1–3′
miR-Universal R primer			5′-R-GTGCAGGGTCCGAGGTAT-3′

F: Forward; R: Reverse; PR: Probe; RT: Reverse Transcriptase.
[a] www.ncbi.nlm.nih.gov/gene.
[b] www.ncbi.nlm.nih.gov/SNP.

brain tissues were determined by Comparative CT method (ΔΔCT) with Real-Time PCR.

2.8. Statistical analysis

The data were expressed as median and mean ± standard deviation. The behavioral study data were analyzed as repeated measures with ANOVA. The other data were analyzed by ANOVA and Kruskal-Wallis tests for comparisons between the groups and Bonferroni-Dunn post-hoc test for comparisons between the subgroups. All statistical analyses were performed using the SPSS software 21 and Statistical software 8.0; and the $P < 0.05$ value was defined as being statistically significant.

3. Results

3.1. Behavioral performance in the rats

The data from open field testing showed that the locomotor activity of the rats was prominently impaired in the O, O + D and O + D + H Groups versus the D, C Groups. The recording of the distance moved and the velocity that the rats moved in 5 min were significantly increased. The check of the distance moved was markedly decreased in the O + D Group compared with the C Group ($P < 0,05$) (Fig. 2A). In addition to this, the check of the velocity was decreased in the O + D Group compared with the four other groups, but just statistical differences were observed between the C and O + D Groups ($P < 0,05$) (Fig. 2B).

Differently, the Morris maze results showed the function of learning ability in rats. On the first four days, the learning ability revealed an obvious dysfunction in O + D rats (Fig. 3A). Throughout the training, the O + D rats required longer times to reach the platform than the other experimental rats. A statistically significant decrease ($P < 0.001$) was determined in four groups (C, D, O and O + D + H) except O + D with a comparison of time to find the average elevation obtained on the day for each group with repeated measurement analysis of variance (Fig. 3B). The value of (O + D) Group, which generated AH with respect to 4th day values, was greater than the C, D, O, O + D + H Groups, and a statistically significant difference ($P < 0,05$) was observed between them (Fig. 3C). A probe test, in which the platform was removed, was accomplished on day 5. The rats spent the majority of their time swimming in the quadrant where the platform was located. No significant differences were found between all the groups (Fig. 3D).

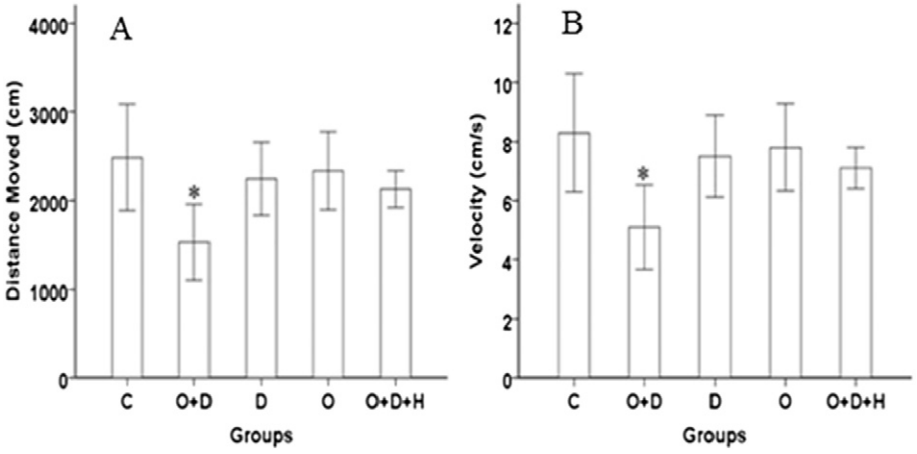

Fig. 2. Impairments of behavioral performance in the 10w O + D Group (A-B) in the open field test, which is different from C (*$P < 0.05$). C = the intact Control Group; O + D = the OVX and D-gal injected Group; O + D + E = the OVX and D-gal injected and Huperzine-A (Hup-A) injected Group; D = sham operation and D-gal injected Group; O = the OVX-only Group.

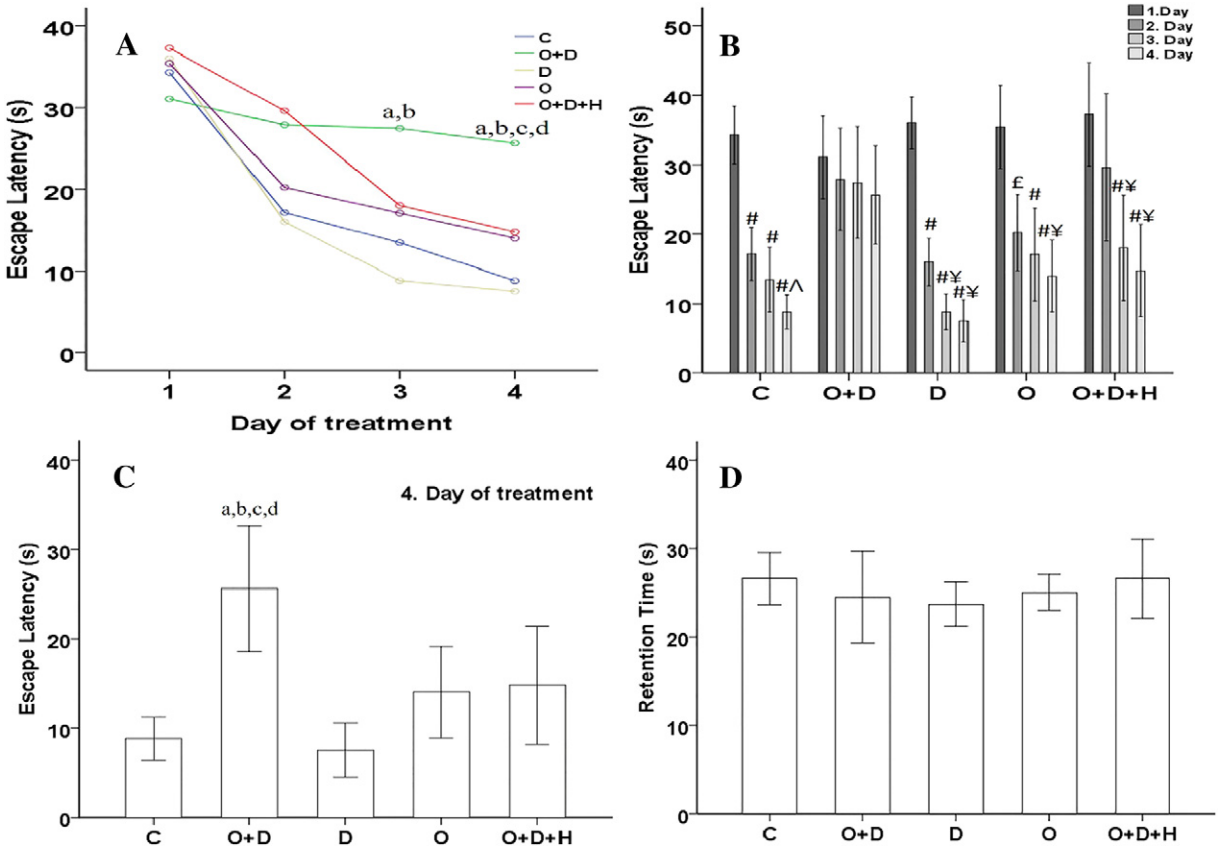

Fig. 3. The water maze test on five experimental groups after D-gal and Hup-A injection. (A) Latencies to platform during 4 training days were significantly different from C $^{a}P < 0.05$, D $^{b}P < 0.05$, O $^{c}P < 0.05$ and O + D + H $^{d}P < 0.05$. (B) Throughout the training, the comparison of latencies day by day for each group was significantly different from 1st Day $^{\#}P < 0.001$ and $^{£}P < 0.05$, 2nd Day $^{\wedge}P < 0.001$ and $^{¥}P < 0.05$. (C) Latency on the last day of the training decreased in the O + D Group compared with the other experiment groups, which was significantly different from C $^{a}P < 0.05$, D $^{b}P < 0.05$, O $^{c}P < 0.05$ and O + D + H $^{d}P < 0.05$. (D) The time spent in the quadrant of the former platform position (means ± SD).

3.2. Electro-biophysical recordings

Based on upregulated β-amyloid peptide (βAP) expression in the Alzheimer disease, β-amyloid peptide can also permeate to peripheral tissues. It was investigated whether ICM, which can develop as a result of the excessive accumulation of βAP in muscle tissue in progressive course of AD and shares many similarities with the pathophysiology of AD, developed or not in the rat model formed with long-term injection of D-galactose after ovariectomy in this study; and also, the effects of dementia occurring in this model on electrical and mechanical activity of the EDL muscle were evaluated.

3.2.1. Compound motor action potentials (CMAPs - EMG) of EDL muscle

The amplitude, total time, area, depolarization time and half-repolarization time of CMAPs in all five groups (Control, D, O + D, O, O + D + H) were measured in Table 2. The differences between the experimental groups were not significant (Table 2).

3.2.2. Mechanical activity data of EDL muscles

3.2.2.1. The force–frequency relationship. Prestresses which bring the muscle to the optimal length were applied to achieve the maximal contractile force in the EDL muscle (Table 3). After appropriate prestresses which bring each EDL muscle to their optimum length were applied to the muscle, stimuli at different frequencies (1 (Twitch) (T_W), 10, 20, 40, 80, 100 and 150 Hz) were given with an interval of 5 min and also the maximum contractile force responses to each stimulus were recorded (Fig. 4). The contraction and half-relaxation times of oscillation curves recorded from the muscles which underwent a single square pulse (0.5 ms duration and supramaximal amplitude) were measured (Fig. 5A and B).

Table 2
Descriptive statistics for CMAPS that were recorded from the EDL muscles (mean ± SD).

	Control ($n = 12$)	O + D ($n = 14$)	D ($n = 14$)	O ($n = 14$)	O + D + H ($n = 14$)	P
Amplitude (mV)	6.200 ± 1.770	7.780 ± 2.610	7.290 ± 1.710	5.970 ± 2.030	7.630 ± 1.500	**0.358**
Total time (ms)	5.090 ± 0.680	4.190 ± 0.880	4.240 ± 1.960	4.010 ± 0.920	4.150 ± 0.640	**0.179**
Area (mV.ms)	0.009 ± 0.003	0.009 ± 0.003	0.007 ± 0.004	0.006 ± 0.003	0.008 ± 0.002	**0.477**
Depolarization time (ms)	1.420 ± 0.440	0.890 ± 0.250	0.870 ± 0.490	0.850 ± 0.440	0.760 ± 0.160	**0.096**
Half-repolarization time (ms)	1.840 ± 0.220	1.650 ± 0.460	1.680 ± 0.810	1.580 ± 0.320	1.690 ± 0.250	**0.634**

Table 3
Descriptive statistics for pre-tension (g) values that were recorded from the EDL muscles for each stimulus protocol.

	Control ($n = 12$)	O + D ($n = 14$)	D ($n = 14$)	O ($n = 14$)	O + D + H ($n = 14$)	P
T_W	2.19 ± 0.31	2.19 ± 0.14	2.09 ± 0.17	2.36 ± 0.23	2.29 ± 0.13	**0.209**
10 Hz	2.12 ± 0.15	2.14 ± 0.10	2.17 ± 0.10	2.14 ± 0.19	2.22 ± 0.16	**0.817**
20 Hz	2.19 ± 0.32	2.11 ± 0.11	2.18 ± 0.08	2.42 ± 0.48	2.13 ± 0.07	**0.237**
40 Hz	2.01 ± 0.09	2.07 ± 0.06	2.12 ± 0.08	2.22 ± 0.94	2.04 ± 0.19	**0.907**
80 Hz	2.12 ± 0.13	2.07 ± 0.10	2.23 ± 0.21	2.25 ± 0.30	2.11 ± 0.07	**0.471**
100 Hz	2.22 ± 0.26	2.01 ± 0.23	2.16 ± 0.15	2.25 ± 0.19	2.04 ± 0.20	**0.205**
150 Hz	2.13 ± 0.04	2.09 ± 0.27	2.29 ± 0.10	2.22 ± 0.13	2.16 ± 0.16	**0.110**

Isometric oscillation curves which were recorded for stimuli at T_W and 150 Hz (0.5 ms duration and supramaximal amplitude) are shown (Fig. 6).

When prestresses which bring the EDL muscle to the optimal length to achieve the maximum contractile force were compared between the groups, it was observed that there was no statistically significant difference between the groups (Table 2). When the contractile forces obtained for each stimulation frequency were compared between the groups, it was observed that there was a statistically significant decrease at all stimulation frequencies in the O + D group compared to the C group in terms of the contractile forces ($p < 0.001$ for Tw-80 Hz, $p < 0.05$ for 100 and 150 Hz). Similarly, there was a statistically significant decrease at all stimulation frequencies in the O group compared to the C group in terms of the contractile forces ($p < 0.001$ for Tw-40 Hz, $p < 0.05$ for 80–150 Hz).

The maximum contractile forces showed a statistically significant increase at 20 and 40 Hz in the O + D + H group compared to the O + D group ($p < 0.05$). The maximum contractile forces showed a statistically significant increase at Tw and 20 Hz in the O + D + H group (treatment group) compared to the O group ($p < 0.05$). Moreover, the maximum contractile forces showed a statistically significant decrease at T_W, 10, 20, 40 and 80 Hz in the D group compared to the C group ($p < 0.05$).

The contraction times of oscillation curves recorded from the groups which underwent a single square pulse (0.5 ms duration and supramaximal amplitude) showed a statistically significant decrease in the O group (27.69 ± 3.53) compared to the C group (38.02 ± 5.40) ($p < 0.05$). Moreover, the measured half-relaxation times showed a statistically significant decrease in the D group (47.08 ± 9.39) and in the O group (48.59 ± 16.1) compared to the C group (81.04 ± 14.06) ($p < 0.05$).

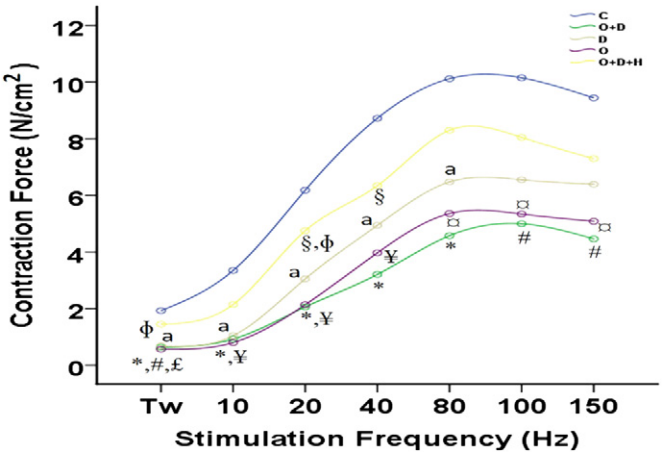

Fig. 4. The recordings of the maximum contraction force curves of the EDL muscle at different stimulation frequencies (Tw, 10, 20, 40, 80, 100 and 150 Hz) for mechanical activity. The O + D group compared to the C group $^{*}p < 0.001$, $^{\#}p < 0.05$. The O group compared to the C group $^{¥}p < 0.001$, $^{¤}p < 0.05$. The O + D + H group compared to the O + D group $^{§}p < 0.05$. The O + D + H group compared to the O group $^{Φ}p < 0.05$. The D group compared to the C group $^{a}p < 0.05$.

3.3. Histopathological evaluation

3.3.1. Neurochemical changes in the brains of the rats

Aβ accumulation showed a statistically significant increase in the O + D group (the group with AD) compared to the C, D and O groups (respectively; $p < 0.001$, $p < 0.001$, $p < 0.001$). βAP accumulation showed a decrease in the O + D + H group (treatment group) compared to the O + D group (the group with AD) but this decrease was not statistically significant ($p = 1.000$) (Fig. 7A). AChE activity in the frontal cortex showed a statistically significant increase in the O + D group compared to other groups ($p < 0.001$). There was a statistically significant difference in the O + D + H group (treatment group) compared to the O + D group (the group with AD) in terms of AChE activity in the frontal cortex ($p < 0.01$) and also AChE activity was not observed in the treatment group and in the C, D and O groups (Fig. 7B).

3.3.2. Neurochemical changes in the EDL muscles of the rats

When βAP accumulation in the EDL muscle of the rats examined for the pathology of ICM was compared between the groups, it was observed that there was no statistically significant difference between the groups ($p = 1.000$) (Fig. 8A). Moreover, when AChE activity in the EDL muscle of the rats was compared between the groups, it was observed that there was no statistically significant difference between the groups ($p = 1.000$) (Fig. 8B).

3.4. Differential expression of miRNAs in AD model rats with the Huperzine-A treatment

In this study, we assessed the expression profiles of five human miRNAs expressions in the Huperzine-A treatment of AD model rats. There was no statistically significant difference between the groups in terms of the expression levels of miR-9 and miR-107 (Table 4). While there was a statistically significant difference between the groups in terms of the expression levels of miR-106 and miR-125 ($p < 0.05$), there was no statistically significant difference between the groups in terms of the expression level of miR-29. There was a statistically significant increase in the O + D + H group compared to the O group in terms of the expression level of miR-106 ($p < 0.05$). There was a statistically significant increase in the O + D + H group compared to the O + D group in terms of the expression level of miR-125 ($p < 0.05$) (Table 5).

4. Discussion

Although the majority of AD patients are characterized by dementia, it has also been associated with non-cognitive symptoms such as motor dysfunctions which appear clinically but the pathological mechanism is not known widely. The modellings formed in the studies of AD are generally stereotactic surgical techniques [19]. However, these modellings are not supportive for all of the underlying pathologic findings of AD. We preferred the rat model of Alzheimer's Disease used in this study in terms of meeting to all hypotheses underlying the disease and forming clinically domino effect. In a study in women with Hormone Replacement Therapy (HRT), the protective effects of estrogen ensured

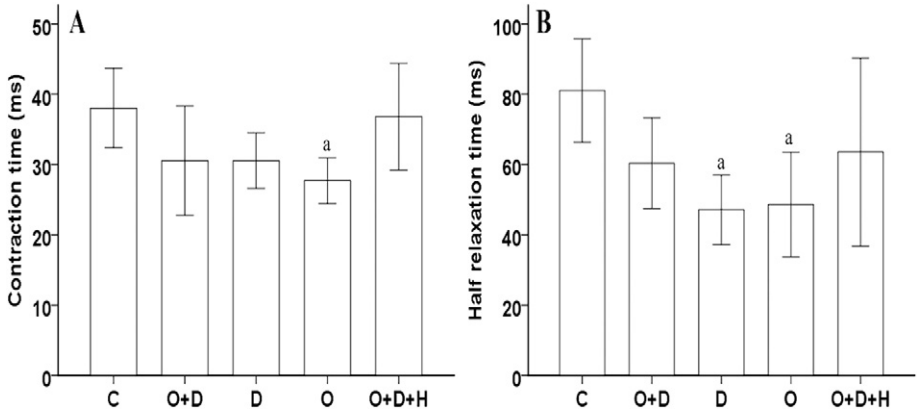

Fig. 5. The effects of bilateral oophorectomy and D-galactose, Huperzine-A treatment on twitch configurations with 95% confidence intervals of the means in rat extensor digitorum longus (A represents the contraction times; and B represents the half-relaxation times). [a]Significantly different from the Control Group. [a]$p < 0.05$.

a delay in the onset of AD and a reduction in the incidence of the disease [20–22]. It was shown that administration of D-galactose led to the free radical formation and also it caused neuronal loss by inducing apoptosis in the hippocampal neurons [23]. Both losses of estrogen and long-term administration of D-galactose increase the production of free radicals by causing metabolic abnormalities, which lead to neuronal damage as a result of these processes. In accordance with this, an AD modeling was developed based on a long-term administration of D-galactose following the formation of menopause by ovariectomy in female Sprague-Dawley rats [13]. We showed that βAP aggregation occurred in the forebrain and AChE activity increased and also skeletal muscle contraction forces decreased at different frequencies in the brain tissue of the rats with bilateral ovariectomy (BOVX) induced with long-term injection of D-galactose, which is a rat model for AD in this study. We found that the effects of Hup-A contributed to the improvement in this process.

In a study conducted on Alzheimer patients, it was reported that the AChE activity, which was determined by using the quantitative Ellman Method, was very high at a significant level in the patient group when compared with the control group [24]. In addition, in another study in which AD rat model was used, it was reported that the AChE activity was increased in the brain tissue when compared with the control group [25–27]. Wan QY [28] conducted another study, and by using the Double Antibody Sandwich Method, determined that there were AChE and ChAT (Choline acetyltransferase) activities in the hippocampus of the brains of the rats in which AD was created. As a result, as the AChE activity increased in the AD group when compared with the control group, the ChAT activity decreased. In another study it was reported that the AChE activity was increased at a statistically significant level in AD rat models [29]. These findings support our findings showing that the AChE activity is high in the Alzheimer Disease group rats.

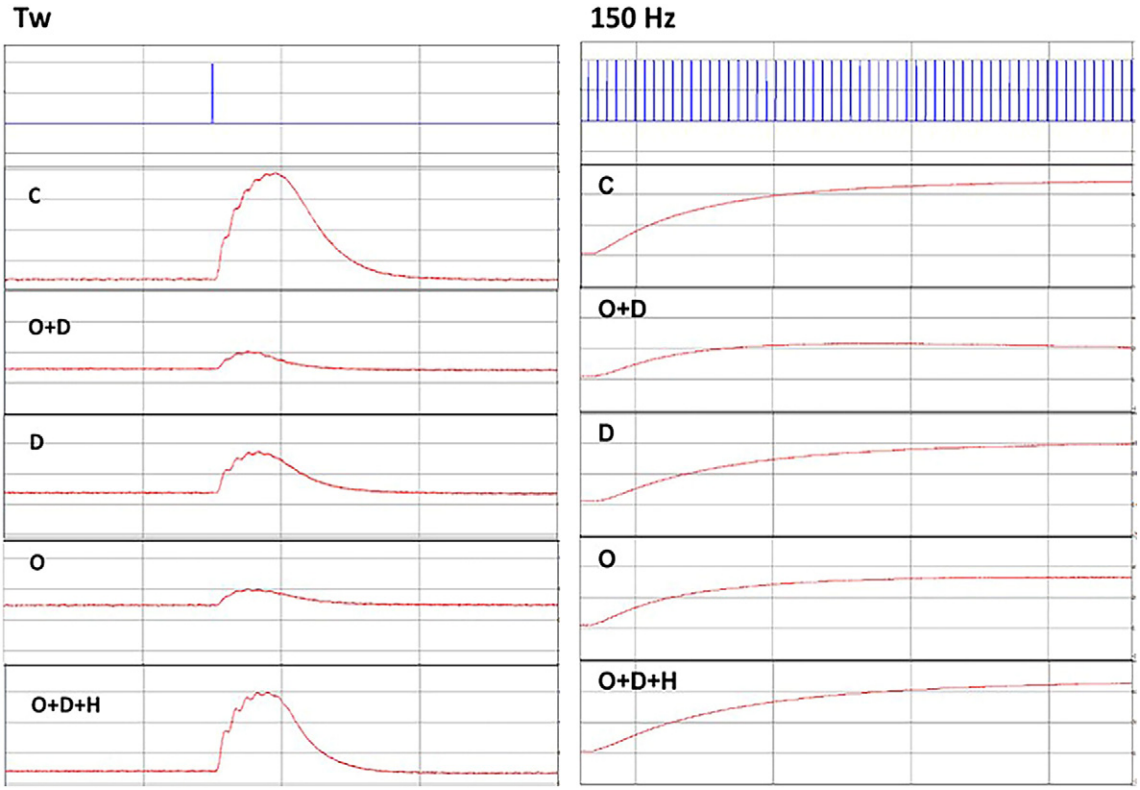

Fig. 6. Sample records of the skeletal muscle mechanical activity in T_W and 150 Hz: the Intact Control group (C); the OVX and D-gal injected Group (O + D); sham operation and D-gal injected Group (D); the OVX-only Group (O); the OVX and D-gal injected and Huperzine-A (Hup-A) injected Group (O + D + H).

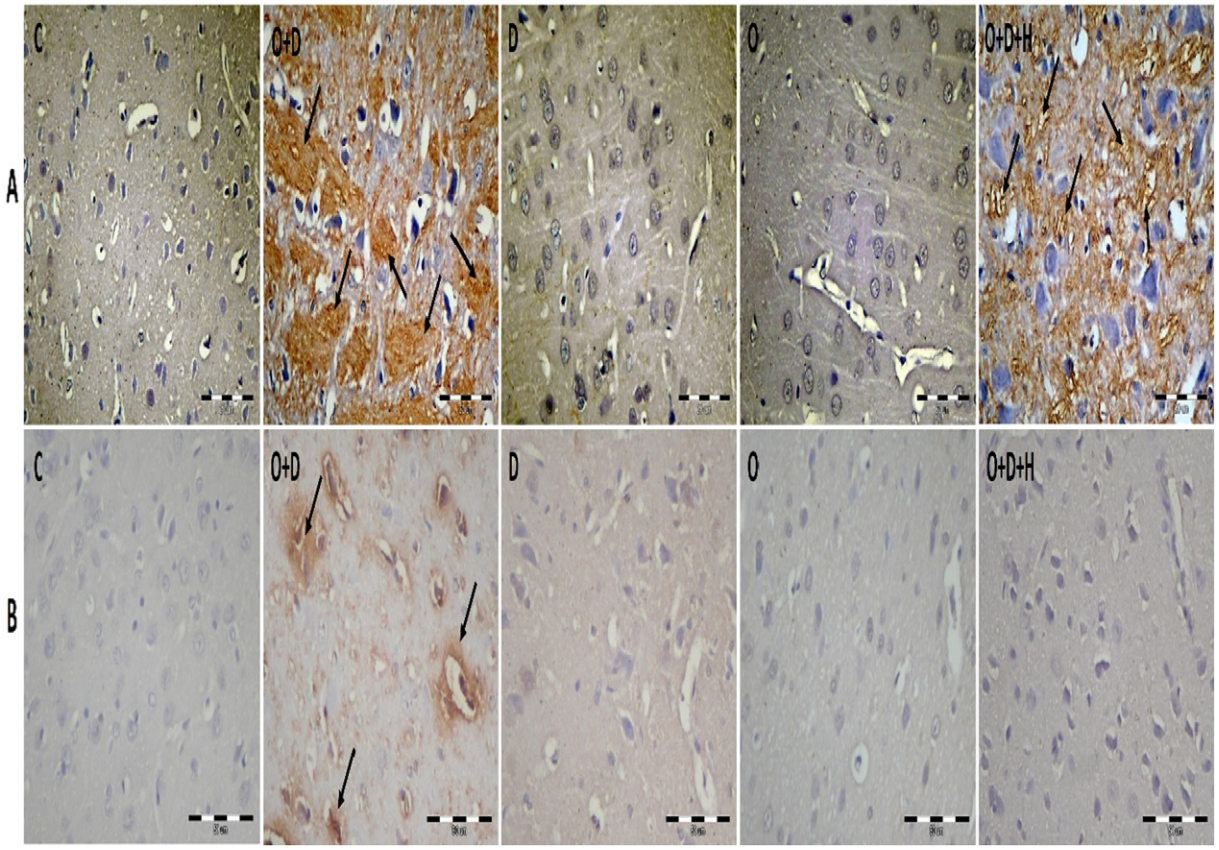

Fig. 7. Aβ expression (A) and AChE activity (B) in the frontal cortex of the rat with immunohistochemical labeling.

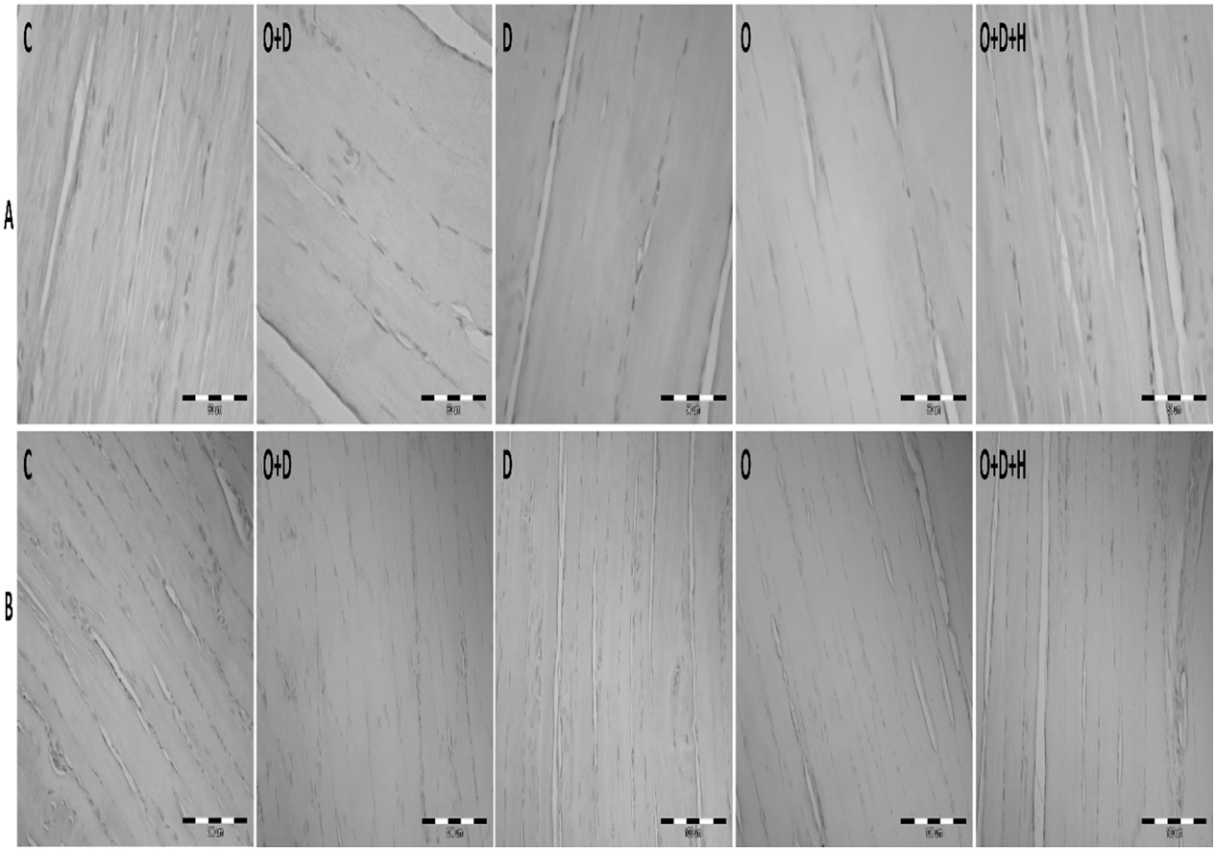

Fig. 8. Aβ expression (A) and AChE activity (B) in the EDL muscle of the rat with immunohistochemical labeling (B).

Table 4
Relationship between *rno-miR-9-5p* and *rno-miR-107* expression levels in the groups.

miRNA	Group	Expression value ($2^{-\Delta\Delta CT}$)	25%	75%	P
rno-miR-9-5p	Control	1.270	0.738	2.857	**0.188**
	O + D	0.595	0.292	2091	
	D	0.724	0.352	1.043	
	O	0.284	0.195	0.375	
	O + D + H	0.848	0.539	1213	
rno-miR-107	Control	3129	0.978	4.598	**0.897**
	O + D	3060	2504	6913	
	D	3175	1879	4225	
	O	1968	1449	2941	
	O + D + H	6548	4800	7517	

However, there are also several other studies showing that the AChE activity decreases. In another study it was reported that the AChE activity decreased for a long duration as a response to specific cholinergic lesion in the AD rat models that were formed with 192 IgG-saporin intraparenchymal injections into the cortical cholinergic field which received input from *bazalis magnosellularis* nucleus [30]. Gil-Bea et al. [31] conducted a study and reported that the acetylcholine (ACh) levels ChAT and AChE activity were decreased in the postmortem frontal cortex in AD group when compared with the control group, and both the ChAT and AChE activities showed a clear correlation with cognitive deficits.

When Hup-A (IC50 = 42 nM) was compared with tacrine (rat-IC50 = 302 nM), donepezil (rat-IC50 = 30 nM) and rivastigmine (rat-IC50 > 10,000 nM) among the drugs which were approved by the FDA for AChE inhibition in the treatment of AD, it was observed that it penetrates better through the blood-brain barrier, it has a higher oral bioavailability and it has longer AChE inhibitory activity [32–34]. Moreover, the side effects of these drugs limit their use in patients with AD. Hup-A reduces both neuronal degeneration and free radical induced oxidative damage caused by βAP in the hippocampus and the cortex and it protects neurons from apoptosis and cytokines generated by βAP and free radicals and also it inhibits glutamate toxicity [35]. In this study, this is the most important reason for the preference of Hup-A to assess its effectiveness in the treatment of AD. βAP-aggregation was observed in the brain frontal cortex in AD rat models. It was found that Hup-A reduced it by dissolving this aggregation.

It is known that Huperzin-A is a reversible AChE inhibitor as one of targets for AD therapy [36]. Peng et al. [36] conducted a study to investigate the effects of Hup-A on the AChE activity, and reported that the AChE activity, which was determined with the Ellman method in the cortexes of the rats with AD model, was high at a significant level when compared with the Control Group, and determined that the AChE activity in the Hup-A group was decreased when compared with the AD group. In our study, the AChE activity, which was determined with the immunohistochemistry method in the frontal cortexes of the rats with AD, was found to be high at a significant level compared to the control group. It was also seen that Hup-A reduced AChE activity. Our results showed very clearly that Hup-A carried out its high AChE inhibitory activity in the rats with AD and played a role in the healing process.

The amyloid cascade hypothesis related to AD is important [37]. Based on the findings in the amyloid cascade hypothesis, it accumulates long and unresolved structures in some other tissues including skin and muscle as in the brain of patients with AD [7]. Amyloid deposits containing same Aβ42 peptide with AD occur in muscles of patients with IBM which is an age-related muscle disease [38]. Moreover, βAP reduced the release of Ca^{+2} through Ca^{+2} channels and therefore reduced the contractions in skeletal muscle in these patients [39].

According to EMG results obtained in this study, there was no statistically significant difference between the groups in terms of the amplitude, area, peak latency and duration of the CMAP. In our study, in the AD modeling formed by Hua et al. [13], βAP accumulation was not seen in the EDL muscle of the rats. Therefore, EMG and histochemical findings support each other. In another study, ovariectomy in rats reduced EMG activity and contractile activity of the genioglossus muscle [40]. In comparison to these findings, the EMG results of our study showed that the bioelectrical properties of the EDL muscle were not sensitive to ovariectomy. In the light of these findings, βAP accumulation did not spread to the peripheral tissues except for the brain tissue in the rat model used. However, it was found that there was a decrease in contractile force measured from oscillation curves recorded from the EDL muscle of the rats for the biomechanical activity of the EDL muscle of the rats. It was understood that our finding occurred as a result of ovariectomy and administration of D-galactose.

In another study supporting that there was a reduction in peak oscillation force recorded from EDL muscle by applying a single square pulse (T_W) in our study, when the values of peak oscillation force for T_W from the skeletal muscle of rats with ovariectomy were compared between the groups, it was observed that it was significantly decreased in ovariectomy group compared to control group [40–41]. The maximum contractile forces of the rats in which AD model was formed and which underwent only ovariectomy and were administered only D-galactose were found to decrease at other stimulation frequencies (10, 20, 40, 80, 100 and 150 Hz). It was found that estrogen deficiency in adult rats caused muscle atrophy [42–43]. It was observed that the muscle strength per unit cross-sectional area decreased in perimenopausal women compared to pre-menopausal women and post-menopausal women receiving HRT [44]. Consequently, there are studies reporting that there was a reduction in muscle function as a result of the removal of the hormones produced by the ovaries and in case of administration of only D-galactose, and also these studies support that a reduction was seen in biomechanical activity in our study. Hup-A raised this reduction to the control levels at certain frequencies (T_W, 20, 40 Hz) in the rats in which AD models were formed and which underwent only ovariectomy, and it was observed that it was an effective treatment.

Patill et al. [45] conducted a study and compared the effects of Hup-A and physostigmin on *rectus abdominus* muscle, phrenic nerve diaphragm slide, ileum and iris sphincter muscle for acetylcholinesterase inhibitor. They found that Hup-A had an acetylcholine-strengthening effect more than the effect of physostigmin on skeleton muscles and increased the acetylcholine activity in the ileum although it was not at a statistically significant level [45]. On the other hand, they also reported that Hup-A had a stronger re-cycling effect than the physostigmin on the neuromuscular block formed with tubocurarine in the phrenic nerve diaphragm slide [45]. Furthermore, they also observed that Hup-A increased the contractile speed in the ileum and the contractile speed of the diaphragm when compared with physostigmin [45]. These findings support our findings claiming that Hup-A has a curative effect on the contractile force in the skeleton muscle.

Table 5
Relationship between rno-miR-29a-5p, rno-miR-106a-5p and rno-miR-125a-3p expression levels in the groups.

miRNA	Control ($2^{-\Delta\Delta CT}$)	O + D ($2^{-\Delta\Delta CT}$)	D ($2^{-\Delta\Delta CT}$)	O ($2^{-\Delta\Delta CT}$)	O + D + H ($2^{-\Delta\Delta CT}$)	P
rno-miR-29a-3p	0.681 ± 0.456	0.270 ± 0.112	0.242 ± 0.137	0.213 ± 0.026	0.495 ± 0.252	**0.074**
rno-miR-106a-5p	6.304 ± 5.078	3.660 ± 1.674	3.107 ± 1.699	1.500 ± 0.659	5.105 ± 1.920	**0.005**
rno-miR-125a-3p	1.061 ± 0.724	0.518 ± 0.142	0.913 ± 0.425	0.752 ± 0.433	1.297 ± 0.355	**0.004**

The open field test was conducted to observe the impairments in locomotor activity in AD in rats with dementia in our study. It was seen that locomotor activity decreased in AD mouse models. Our result is supported by the results of open field test made by Hua et al. [13] who formed AD model. After the rats underwent bilateral ovariectomy, administration of D-galactose caused anxiety symptoms.

Function impairments were seen in AD rat models for the first 4 days (learning process) in the Morris Water Maze test performed to assess spatial memory in this study. Finding times for the average altitude were decreased in the other experimental groups except for AD rat models. The altitude was removed to confirm that the rats learned to find the location of the altitude on the 5th day of the spatial memory test and to show that this was not a coincidence. There was no difference between the rats in the time spent in the south-western quadrant where the altitude was formerly on the 5th day experiment (recall experiment). In a study of Hua et al. [46], when the platform was removed, the time spent in the quadrant where the platform was formerly was lower in AD rat models compared to the others group. When all parameters of finding time for the average altitude within the first 4 days and the time spent in the south-western quadrant were evaluated together, although AD rat models exhibited behavior appropriate to the pathology of AD for only the first 4 days (learning process), it could not be seen on the last day.

As a result of histological examinations, the presence of βAP accumulation in the forebrain of the rats supports impairments in locomotor activity. However, the absence of βAP accumulation in the hippocampus supports the findings obtained on the 5th day of the Morris Water Maze test.

In our study, administration of Hup-A is effective for *rno-miR-106b-5p* and *rno-miR-125a-3p*. However, it did not provide a change in the expression levels of *rno-miR-9-5p, rno-miR-29a-3p* and *rno-miR-107*. miRNAs usually attempt to down-regulate the expression of genes. The expressions of selected miRNAs were decreased in AD brain tissue. The miRNAs that were selected are specific to the brain, and they have possible effects on AH [47]. In previously conducted studies, it was reported that the miR-9, miR-29a, miR-29b, and miR-107 expressions decreased, which led to excessive Aβ accumulation in human and rat brains with AD [48–49]. In a study conducted on Alzheimer patients it was found that the hsa-miR-9-5p, hsa-miR-106a-5p, hsa-miR-106b-5p, and hsa-miR-107 expressions were down-regulated at a significant level [47]. This finding supports our findings claiming that rno-miRNA-106a-5p expression decreased in AD rat model group although it was not at a statistically significant level. In addition, it was found in our study that the rno-miRNA-106a-5p expression, which was down-regulated in our study, was up-regulated by Hup-A in the treatment group. Yilmaz et al. [47] conducted a study on Alzheimer Patients for hsa-miRNA-125a-3p expression, and found that there were no statistically significant differences between the patient group and the controls. In our study, the lack of statistically significant differences between the Alzheimer group and the control group in terms of *rno-miRNA-125a-3p* expression confirms this finding. In addition, in our study, it was shown that Hup-A increased the *rno-miRNA-125a-3p* expression at a statistically significant level compared to the Alzheimer group. In this study, it was also found that Hup-A up-regulated the miRNA expressions in question at a certain level. In the light of these findings, the change of these levels with administration of Hup-A ensures miRNA control again. Thus, Aβ accumulation can be reduced or prevented with the normal function of the target gene. Because this mechanism runs through mRNA, RNA half-life or microRNA-mRNA duplex stability properties and dose selection may influence these results.

A rodent model of AD pathology was formed in this study. It was revealed that whether skeletal muscle dysfunctions which are thought to be associated with AD in this model developed or not, and also the findings were obtained from the analysis of expression levels of down-regulated miRNAs after administration of Hup-A. βAP aggregation was shown to be significantly increased in the frontal cortex of AD rat models. Impairments in locomotor activities and spatial memory functions (the first 4 days) in AD rat models were observed with the behavior experiments. It was determined that estrogen deprivation and oxidative stress led to the pathological development of AD and also it caused a loss of function in the peripheral tissues with electrobiophysical and histopathological changes. Moreover, it was found that Hup-A has a healing effect in AD rat models.

In summary, this study demonstrated that βAP plaques aggregation determined in the frontal cortex were not seen in the hippocampus, the dentate gyrus and the EDL muscle in histopathological examination. Therefore, it was thought that estrogen deprivation and oxidative stress generated by D-galactose caused a reduction in the maximum contractile force in AD rat models. As a result of administration of Hup-A in AD rat models, it was found that βAP plaques in frontal cortex decreased and the maximum contractile force in the EDL muscle increased. Also, it was seen that the expressions of miRNAs which regulate gene expression could be controlled by Hup-A.

In the light these findings of this study, rats should be composedly allowed to age after the completion of administration of D-galactose or administration-time and/or dosage of D-galactose should be increased in studies that will be performed to observe molecular substructure of the model used in the study in all anatomical areas of the brain in AD dementia and to ensure the reflection of the pathologies in the peripheral tissues.

5. Conclusions

In conclusion, it seems that the Hup-A treatment in Alzheimer's disease decreases AChE activity and may reduce βAP plaques aggregation by restoring miRNA regulation and represents a possible option for preventive treatment against possible muscle dysfunction in Alzheimer's disease.

Disclosure/conflicts of interest

The authors declare that there are no conflicts of interest.

Acknowledgements

This study was supported by Mersin University Science and Research Foundation (BAP-SBE BFB (CHT) 2013-1 YL).

References

[1] K. Hsiao, P. Chapman, S. Nilsen, C. Eckman, Y. Harigaya, S. Younkin, F. Yang, G. Cole, Correlative memory deficits, Aβ elevation, and amyloid plaques in transgenic mice, Science 274 (1996) 99–102.
[2] K.M. Webber, R. Bowen, G. Casadesus, G. Perry, C.S. Atwood, M.A. Smith, Gonadotropins and Alzheimer's disease: the link between estrogen replacement therapy and neuroprotection, Acta Neurobiol. Exp. 64 (2004) 113–118.
[3] Y.M. Kuo, T.A. Kokjohn, M.D. Watson, A.S. Woods, R.J. Cotter, L.I. Sue, W.M. Kalback, M.R. Emmerling, T.G. Beach, A.E. Roher, Elevated Aβ42 in skeletal muscle of Alzheimer disease patients suggests peripheral alterations of AβPP metabolism, Am. J. Pathol. 156 (2000) 797–805.
[4] G. Vattemi, A. Nogalska, E.W. King, C. D'Agostino, F. Checler, V. Askanas, Amyloid-β42 is preferentially accumulated in muscle fibers of patients with sporadic inclusion-body myositis, Acta Neuropathol. 117 (2009) 569–574.
[5] P.M. Roos, O. Vesterberg, M. Nordberg, Inclusion body myositis in Alzheimer's disease, Acta Neurol. Scand. 124 (2011) 215–217.
[6] M.A. Mukhamedyarov, S.N. Grishin, E.R. Yusupova, A.L. Zefirov, A. Palotás, Alzheimer's β-amyloid-induced depolarization of skeletal muscle fibers: implications for motor dysfunctions in dementia, Cell. Physiol. Biochem. 23 (2009) 109–114.
[7] M.A. Mukhamedyarov, A.Y. Teplov, S.N. Grishin, A.V. Leushina, A.L. Zefirov, A. Palotás, Extra neuronal toxicity of Alzheimer's β-amyloid peptide: comparative study on vertebrate skeletal muscles, Muscle Nerve 43 (2011) 872–877.
[8] M.A. Mukhamedyarov, E.M. Volkov, A.V. Leushina, Y.O. Kochunova, A. Palotás, A.L. Zefirov, Ionic and molecular mechanisms of β-amyloid-induced depolarization in mouse skeletal fibers, Neurosci. Behav. Physiol. 43 (2013) 479–484.
[9] S.S. Hebert, Macro roles for microRNAs in the life and death of neurons, Springer-Verlag Berlin Heidelberg, Berlin, 2010 91–96 Hardcover, Chapt. 10.
[10] G. Yang, Y. Wang, J. Tian, J.P. Liu, Huperzine A for Alzheimer's disease: a systematic review and meta-analysis of randomized clinical trials, PLoS One 8 (2013), e74916. .

[11] J. Patocka, Huperzine A - an interesting anticholinesterase compound from the Chinese herbal medicine, Acta Med. Austriaca 41 (1998) 155–157.
[12] C.A. Frye, J.D. Sturgis, Neurosteroids affect spatial/reference, working, and long term memory of female rats, Neurobiol. Learn. Mem. 64 (1995) 83–96.
[13] X. Hua, M. Lei, Y. Zhang, J. Ding, Q. Han, G. Hu, M. Xiao, Long-term D-galactose injection combined with ovariectomy serves as a new rodent model for Alzheimer's disease, Life Sci. 80 (2007) 1897–1905.
[14] L. Luques, S. Shoham, M. Weinstock, Chronic brain cytochrome oxidase inhibition selectively alters hippocampal cholinergic innervation and impairs memory: prevention by ladostigil, Exp. Neurol. 206 (2007) 209–219.
[15] M.J. Aminoff, Electromyography in Clinical Practice, 3, Churchill Livingstone Edinburgh, 1998 113–145.
[16] C. Souccar, L.M.T. Lima, G. Ballejo, A.J. Lapa, Mechanism of neuromuscular blockadeinduced by phenthonium, a quaternary derivative of (−)-hyoscyamine, in skeletal muscles, Br. J. Pharmacol. 124 (1998) 1270–1276.
[17] G. Orliaguet, O. Langeron, C. Coirault, S. Fratea, P. Coriat, B. Riou, Effects of dantrolene on rat diaphragm muscle during postnatal maturation, Anesthesiology 94 (2001) 468–474.
[18] M.B. Avison, Measuring gene expression, Taylor and Francis Group, New York, 2007 pp. 56-56 Chapt. 2.
[19] I.T. Uzbay, Alzheimer Hastalığına Yönelik Çalışmalarda Kullanılan Deneysel Hayvan Modelleri, Demans Dergisi 1 (2003) 5–14.
[20] C. Kawas, S. Resnick, A. Morrison, R. Brookmeyer, M. Corrada, A. Zonderman, C. Bacal, D.D. Lingle, E. Metter, A prospective study of estrogen replacement therapy and the risk of developing Alzheimer's disease: the Baltimore Longitudinal Study of Aging, Neurology 48 (1997) 1517–1521.
[21] M.X. Tang, D. Jacobs, Y. Stern, K. Marder, P. Schofield, B. Gurland, H. Andrews, R. Mayeux, Effect of oestrogen during menopause on risk and age at onset of Alzheimer's disease, Lancet 348 (1996) 429–432.
[22] V.W. Henderson, H.A. Paganini, C.K. Emanuel, M.E. Dunn, J.G. Buckwalter, Estrogen replacement therapy in older women. Comparisons between Alzheimer's disease cases and nondemented control subjects, Arch. Neurol. 51 (1994) 896–900.
[23] D.H. Chui, H. Tanahashi, K. Ozawa, S. Ikeda, F. Checler, O. Ueda, H. Suzuki, W. Araki, H. Inoue, K. Shirotani, K. Takahashi, F. Gallyas, T. Tabira, Transgenic mice with Alzheimer presenilin 1 mutations show accelerated neurodegeneration without amyloid plaque formation, Nat. Med. 5 (1999) 560–564.
[24] P. Atukeren, M. Cengiz, H. Yavuzer, R. Gelisgen, E. Altunoglu, S. Oner, F. Erdenen, D. Yuceakın, H. Derici, U. Cakatay, H. Uzun, The efficacy of donepezil administration on acetylcholinesterase activity and altered redox homeostasis in Alzheimer's disease, Biomed Pharmacother 90 (2017) 786–795.
[25] H.F. Aly, F.M. Metwally, H.H. Ahmed, Neuroprotective effects of dehydroepiandrosterone (DHEA) in rat model of Alzheimer's disease, Acta Biochim. Pol. 58 (2011) 513–520.
[26] O.J. Olajide, E.O. Yawson, I.T. Gbadamosi, T.T. Arogundade, E. Lambe, K. Obasi, I.T. Lawal, A. Ibrahim, K.Y. Ogunrinola, Ascorbic acid ameliorates behavioural deficits and neuropathological alterations in rat model of Alzheimer's disease, Environ. Toxicol. Pharmacol. 50 (2017) 200–211.
[27] Z. Mokhtari, T. Baluchnejadmojarad, F. Nikbakht, M. Mansouri, M. Roghani, Riluzole ameliorates learning and memory deficits in Aβ25-35-induced rat model of Alzheimer's disease and is independent of cholinoceptor activation, Biomed Pharmacother 87 (2017) 135–144.
[28] Q.Y. Wan, Effect of Dipsacus total saponins on the ability of learning and memory and acetylcholine metabolism of hippocampus in AD rats, Zhongguo Ying Yong Sheng Li Xue Za Zhi. 31 (2015) 82–84.
[29] H. Sohanaki, T. Baluchnejadmojarad, F. Nikbakht, M. Roghani, Pelargonidin improves memory deficit in amyloid β25-35 rat model of Alzheimer's disease by inhibition of glial activation, cholinesterase, and oxidative stress, Biomed Pharmacother 83 (2016) 85–91.
[30] C. Szigeti, N. Bencsik, A.J. Simonka, A. Legradi, P. Kasa, K. Gulya, Long-term effects of selective immunolesions of cholinergic neurons of the nucleus basalis magnocellularis on the ascending cholinergic pathways in the rat: a model for Alzheimer's disease, Brain Res. Bull. 94 (2013) 9–16.
[31] F.J. Gil-Bea, M. Garcı'a-Alloza, J. Dominguez, B. Marcos, M.J. Ramirez, Evaluation of cholinergic markers in Alzheimer's disease in a model of cholinergic deficit, Neurosci. Lett. 375 (2005) 37–41.
[32] R. Wang, H. Yan, X.C. Tang, Progress in studies of huperzine A, a natural cholinesterase inhibitor from Chinese herbal medicine, Acta Pharmacol. Sin. 27 (2006) 1–26.
[33] Y. Zhao, J. Dou, T. Wu, H.A. Aisa, Investigating the antioxidant and acetylcholinesterase inhibition activities of Gossypium herbaceam, Molecules 18 (2013) 951–962.
[34] R. Jackisch, S. Förster, M. Kammerer, A.K. Rothmaier, A. Ehret, J. Zentner, T.J. Feuerstein, Inhibitory potency of choline esterase inhibitors on acetylcholine release and choline esterase activity in fresh specimens of human and rat neocortex, J. Alzheimers Dis. 16 (2009) 635–647.
[35] K.A. Wollen, Alzheimer's disease: the pros and cons of pharmaceutical, nutritional, botanical, and stimulatory therapies, with a discussion of treatment strategies from the perspective of patients and practitioners, Altern. Med. Rev. 15 (2010) 223–244.
[36] L. Peng, Z. Rong, H. Wang, B. Shao, L. Kang, H. Qi, H. Chen, A novel assay to determine acetylcholinesterase activity: The application potential for screening of drugs against Alzheimer's disease, Biomed. Chromatogr. (2017) http://dx.doi.org/10.1002/bmc.3971.
[37] M.S. Parihar, T. Hemnani, Alzheimer's disease pathogenesis and therapeutic İnterventions, J. Clin. Neurosci. 11 (2004) 456–467.
[38] V. Askanas, W.K. Engel, Inclusion-body myositis: muscle-fiber molecular pathology and possible pathogenic significance of its similarity to Alzheimer's and Parkinson's disease brains, Acta Neuropathol. 6 (2008) 583–595.
[39] A. Shtifmana, C.W. Ward, D.R. Laver, M.L. Bannisterd, J.R. Lopez, M. Kitazawa, F.M. Ferla, N. Ikemoto, H.W. Querfurth, Amyloid-β protein impairs Ca^{2+} release and contractility in skeletal muscle, Neurobiol. Aging 31 (2010) 2080–2090.
[40] Y. Liua, S. Jiab, Y. Hou, Effects of Ovariectomy on rat genioglossal muscle contractile properties and fiber-type distribution, Angle Orthod. 79 (2009) 509–514.
[41] Y. Hou, S. Jia, Y. Liu, 17b-estradiol accentuates contractility of rat genioglossal muscle via regulation of estrogen receptor α, Arch. Oral Biol. 55 (2010) 309–317.
[42] M. Kobori, T. Yamamuro, Effects of gonadectomy and estrogen administration on rat skeletal muscle, Clin Orthop. 243 (1989) 306–311.
[43] S. Suzuki, T. Yamamuro, Long-term effects of estrogen on rat skeletal muscle, Exp. Neurol. 87 (1985) 291–299.
[44] S. Phillips, K.M. Rook, N.C. Siddle, S.A. Bruce, R.C. Woledge, Muscle weakness in women occurs at an earlier age than in men, but strength is preserved by hormone replacement therapy, Clin. Sci. 84 (1993) 95–98.
[45] K.D. Patil, R.A. Buerki, P.N. Patil, Potentiation of acetylcholine action by huperzine-A and physostigmine on some vertebrate effectors, including human iris sphincter muscle, J. Ocul. Pharmacol. Ther. 19 (2003) 135–143.
[46] X. Hua, M. Lei, J. Ding, Q. Han, G. Hu, M. Xiao, Pathological and biochemical alterations of astrocytes in ovariectomized rats injected with D-galactose: a potential contribution to Alzheimer's disease processes, Exp. Neurol. 210 (2008) 709–718.
[47] S.G. Yilmaz, M.E. Erdal, A.A. Ozge, M.A. Sungur, Can peripheral MicroRNA expression data serve as Epigenomic (upstream) biomarkers of Alzheimer's disease? OMICS A. J. Integr. Biol. 20 (2016) 456–461.
[48] S.S. Hebert, K. Horre, L. Nicolai, B. Bergmans, A.S. Papadopoulou, A. Delacourte, B. De Strooper, MicroRNA regulation of Alzheimer's amyloid precursor protein expression, Neurobiol. Dis. 33 (2009) 422–428.
[49] W.X. Wang, Q. Huang, Y. Hu, A.J. Stromberg, P.T. Nelson, Patterns of microRNA expression in normal and early Alzheimer's disease human temporal cortex: white matter versus gray matter, Acta Neuropathol. 121 (2011) 193–205.